Stardom University

Stardom Scientific Journal of Natural and Engineering Sciences

- Stardom Scientific Journal of Natural and Engineering Sciences -
Peer Reviewed Scientific Journal published twice
a year by Stardom University

1st issue- 4th Volume 2026

ISSN 3756-2980

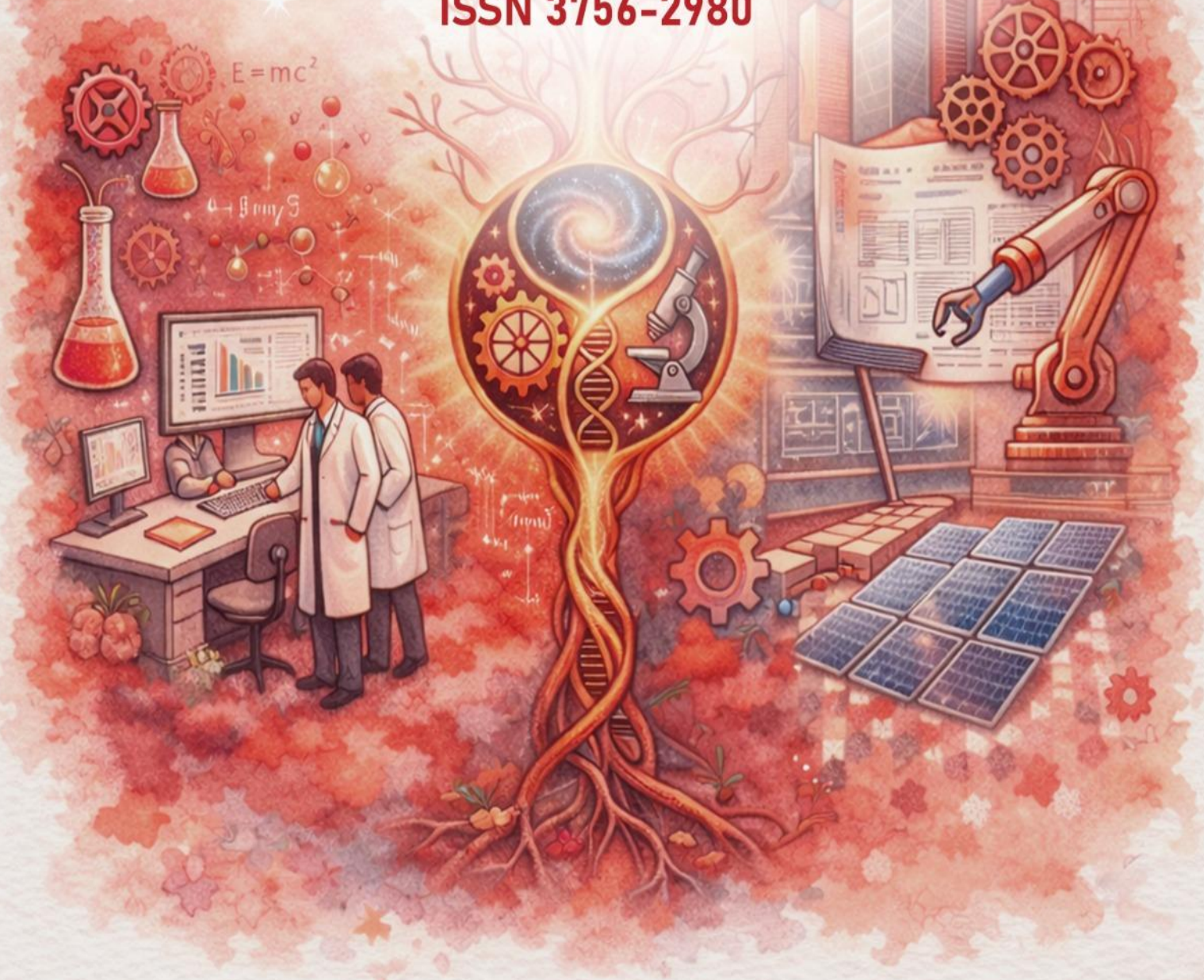

Stardom Scientific Journal of Natural and Engineering Sciences
Peer Reviewing Committee

Editor in Chief

Prof. Sayed Hemeda- Egypt

Editorial Board Manager

Associ. Prof. Dr. Redwan Mohammed Saad – Yemen

Editorial board members

Prof. Chongqing- China

Prof. Antonio Zanutta– Italy

Associ. Prof. Amin Beiranvand Pour- Malysia

Prof. Maria Stefanidou- Greece

DR. Ahmed Mohsen Hassan Metwally- Egypt

Alaa Ibrahem Mohamed Ali- Egypt

Consultency Committee

Dr. Taha A. Elwi- Iraq

All Rights are reserved by Stradom Scientific Journal of Natural and Engineering Sciences

Investigative Insights into Construction Materials of Oraby Tabia, Egypt: Addressing Durability Challenges through Multidimensional Analysis

Mohammed Hamid[1]*, Yosr Elsayed[1], Sayed Hemeda[2]

*Corresponding Author and 1. Conservation Department, Faculty of Archaeology, Damietta University. Damietta, Egypt.
2. Architectural Conservation Department, Faculty of Archaeology, Cairo University, Giza, Egypt.
Sayed.hemeda@cu.edu.eg Tel: 002 0237200960. Fax: 002 35728108
ORCID ID: https://orcid.org/0000-0003-0308-9285

Abstract

This study explores the degradation of construction materials used in Oraby Tabia (OT) buildings through a series of chemical, physical, mechanical, and microbial analyses. Scanning Electron Microscopy (SEM) revealed surface deterioration attributed to environmental factors. Chemical characteristics were assessed via X-ray Diffraction (XRD) and Energy Dispersive X-ray (EDX) spectroscopy, aiding in the selection of materials for potential conversion. Physical testing demonstrated that bricks had a higher absorption rate (11.8%) compared to rocks (5.1%), while exhibiting lower porosity and saturation factors. Mechanical property evaluations indicated significant variability linked to the sample locations. Microbial analysis revealed the highest bacterial load on wood surfaces, with E. coli and Bacillus sp. detected across all samples. Notably, Clostridium sp. was exclusively identified on wood, indicating the necessity for targeted treatments to mitigate microbial degradation. These findings underscore the importance of material selection and preservation in the conservation of architectural integrity.

1. Introduction

The Urabi Fort, known locally as Tabia Oraby (TO), is strategically situated in Ezbet El-Borg, a coastal city in the Damietta Governorate of Egypt. It occupies the eastern bank of the Nile River at the very point where the Damietta branch flows into the Mediterranean Sea. This location places it directly opposite the resort town of Ras El-Bar, giving it a commanding view and control over the waterway's northern entrance. The TO's ruins are now considered a key archaeological and heritage feature of the Ezbet El-Borg waterfront, signifying its enduring physical and cultural presence in the region [1-3].

The TO's primary importance has always been its military and defensive function. For centuries, the mouth of the Nile at Damietta was a vulnerable point for naval invasions, making coastal fortifications essential for national security. The TO be a critical component of this defensive system, designed to control river traffic, repel enemy warships, and protect the Egyptian coastline from maritime incursions. Its role as a key defensive stronghold is well-documented in military histories, which underscore its value in safeguarding one of Egypt's most vital economic and strategic waterways from foreign naval power [4].

While fortifications existed at this location since at least the 18th century, the TO's modern identity and name are inextricably linked to the Egyptian nationalist movement of the late 19th century. It became famously associated with Colonel Ahmed Urabi and the Urabi Revolt (1879-1882), an uprising against the Khedive's government and growing European influence. During this period, the TO be a symbol of national sovereignty and a key bastion in the defense against the anticipated British intervention. Because of its role in this pivotal anti-colonial struggle, the TO is remembered not just as a military structure, but as a monument to Egyptian resistance [5].

TO be officially registered as an Islamic monument under Decree No. 21 of 1985, dated January 17, 1985, under the designation “TO in Ezbet El-Borg.” This decree

was published in the Egyptian Official Gazette, Issue No. 73, on March 29, 1985. TO is one of the most significant archaeological sites in Damietta Governorate. Built by the French in the 18th century, the TO gained further prominence during Mohammed Ali's reign. It became known as the TO after being occupied by Urabi soldiers during the British occupation of Egypt. The TO was primarily used for military defense against naval invasions. However, it has suffered significant deterioration due to neglect and human damage, leading to the loss of many of its parts. Few studies have been conducted to restore and develop the TO. [6].

Fig.1. Features of the main buildings of Tabia Oraby.

2. Geographical and Architectural Descriptions

Northern Boundary

The current protective wall delineates the northern boundary of the designated heritage zone. A primary school and food processing factory are located in close proximity to each other. In the event of future removal, a buffer zone of 20 meters must be preserved.

Southern Boundary

The protective wall also defined the southern boundary of the site. The area contains infrastructure, including sewage and water pipelines, as well as burial grounds. Should demolition occur, a 20-meter buffer zone is required

Eastern Boundary

The existing protective wall marks the eastern perimeter of this site. The adjacent land has been allocated to a youth center and a five-a-side football field by the Damietta Governorate, as per Allocation Decree No. 16 of 2009. Additionally, there are nearby Muslim cemeteries. A buffer zone of 20 m must be maintained in the event of structural removal.

Western Boundary

The Nile riverbank constitutes a natural protective buffer. It is important to note the presence of a secondary school in the southwestern section, which was constructed prior to the site's official registration. Furthermore, the area includes shipbuilding and repair workshops, for which a removal order was issued under Decree No. 3170, dated November 7, 2006.

The TO adopts an incomplete star-shaped layout and is composed of two defensive walls: an outer wall, approximately one meter thick, constructed of fired brick and stone, and an inner wall built entirely of fired bricks. Between the two walls lies a ditch that was historically filled with water through channels connected to the Nile. The main entrance to the TO is situated along the southern side of the outer wall; however, it has collapsed, leaving only the remains of the left shoulder of the entrance block, which was made of limestone.

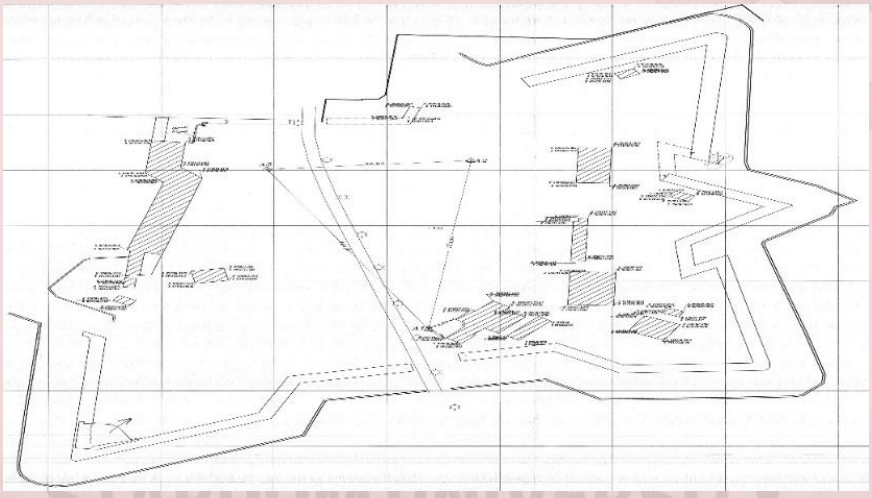

Fig. 4.2. Tabia Oraby layout.

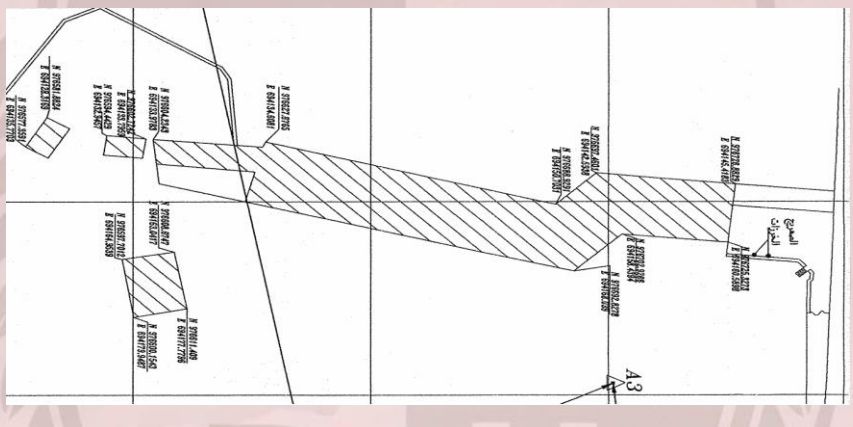

Fig. 3. The main structure of the Tabia Oraby (military barracks).

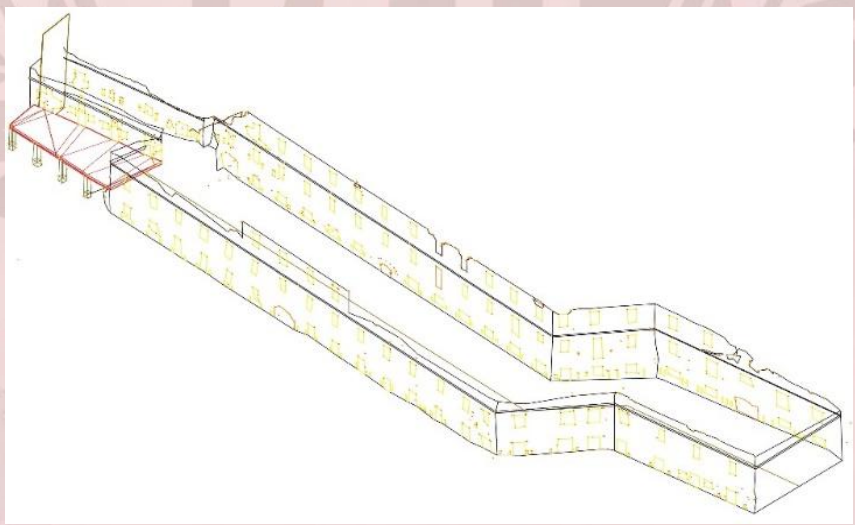

Fig. 4. 3D view of the degradation map for the Tabia Oraby (military barracks).

This surviving section projects approximately one meter beyond the wall, while the rest of its features have disappeared beneath a modern road that now cuts across the site, dividing it into two sections.

The eastern section contains several architectural units and ammunition depots, in addition to the Sidi al-Maghribi Mosque, which was recently removed from the register of protected monuments. The western section contains the residence of the Hakimdar (the TO's commander), the Qishlaq building (soldiers' barracks), as well as storage facilities and water cisterns building.

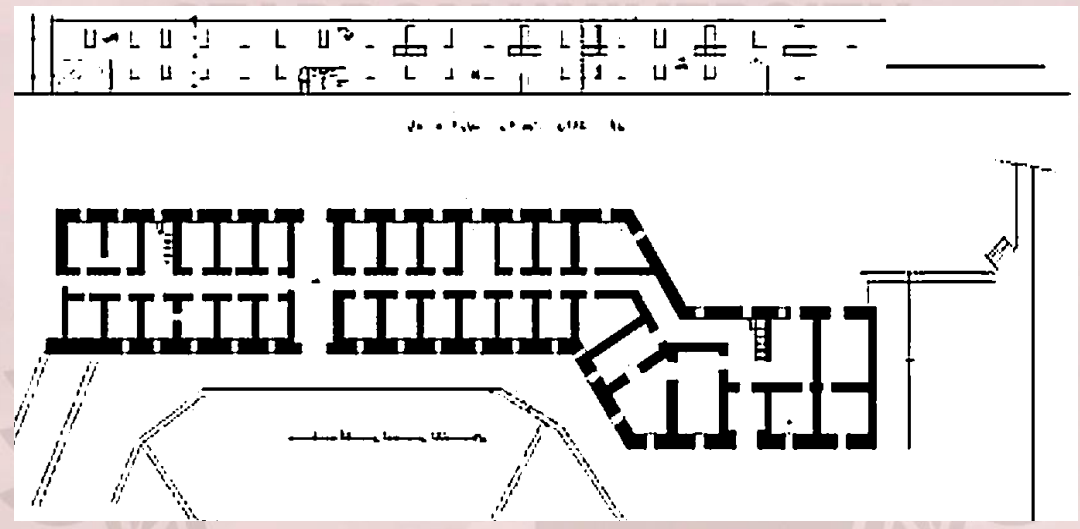

Fig. 5. Plan view for original dimensions

Historic sites, like the TO, embody cultural identity and collective memory as remnants of past civilizations and respective accomplishments. They include the historical record, architectural achievement, and societal values of the previous era, and they tell a story that can teach us immensely beyond their use as monuments to the past [7]. Also, in many cases, these sites have considerable economic potential to contribute largely to a local economy through tourism, presenting a unique experience to visitors while generating income for the site and local economy [8]. As a result, maintaining these structures is not simply about preserving physical artifacts of buildings, but about cultural continuity, historical knowledge, and sustainable development for coming generations.

Nonetheless, certain cultural treasures cannot be replaced and are in constant danger of deterioration by a variety of threats, including deteriorating environmental agents, natural disasters, or human causes. The TO and its significance as a historical structure is an example of this condition, as the TO has degenerated considerably through neglect and contamination from environmental forces[9]. Determining the mechanism or causes of deterioration

is crucial to studying specific types of deterioration, whether they be physical, chemical, mechanical, or microbiological. That study provides the scientific foundation to develop evidence-based programs for conservation and rehabilitation-helpful for determining how to intervene structurally with awareness of the integrity of the structure and heritage preservation standards [10-12].

A series of representative samples was randomly extracted from various structural elements and locations within the building to ensure comprehensive coverage of the construction materials. The sampling process included six brick samples for stress strain analysis, aimed at determining their elastic modulus and deformation characteristics under loading, as well as five additional brick specimens prepared for uniaxial compression testing to accurately assess their compressive strength and load-bearing capacity. This approach was designed to capture the variations in the material quality across different areas of the structure. All specimens were subjected to a comprehensive laboratory testing program encompassing mechanical, physical, and microbiological analyses.

Mechanical testing focuses on quantifying strength parameters and identifying signs of degradation, whereas physical analysis investigates material composition, the presence of harmful salts, and other factors contributing to deterioration. In parallel, microbiological testing is performed on selected samples to detect and characterize bacterial and fungal activity that may accelerate biodeterioration processes, such as acid production, salt crystallization, and the weakening of bonding agents. The combined results of these multidisciplinary investigations will provide critical insights into the current condition of the building's structural components, inform evidence-based conservation or rehabilitation strategies, and ensure that any interventions align with relevant engineering and heritage preservation standards.

3. Materials and Methods

3.1 Sample Collection and Origin

Samples of constituent building materials were gathered from the TO historic site in Ezbet El-Borg in Damietta. The samples included bricks, building stones, binding mortar, and structural wooden components. The samples were selected on the basis that all would represent the original TO's early construction.

3.2 Visual and Morphological Characterization

All samples were subject to a detailed visual inspection to record their physical and morphological characteristics under the categories of color, texture, surface characteristics, evidence of manufacture, and evidence of degradation. Where possible, color descriptions were made using a standardized color chart for objectivity, and all observations were made under the same laboratory lighting.

3.3 SEM and EDX analyses

The surface morphology of historical parts of TO, including bricks, wood, stone, and mortars, was examined using a scanning electron microscope (JEOL JSM-6510LB, Tokyo, Japan) to study their microstructure, composition, and deterioration patterns for these materials. In addition, the decay and weathering were assessed using SEM analysis to make an accurate prediction for the current condition and durability of these materials and to predict how long these structures can endure. Additionally, EDX analysis was conducted to analyze the chemical elements found on the surfaces of the tested samples of TO using an energy dispersive spectroscopy unit equipped to a scanning electron microscope.

3.4 X-ray Diffraction (XRD) Analysis

The brick, stone, and mortar samples were examined using X-ray Diffraction (XRD) analysis using an Empyrean series 3 X-ray diffraction instrument (PANalytical) to determine the mineralogical composition of the inorganic materials. Using a mortar and pestle, representative amounts of each sample were manually ground into a fine, uniform powder before examination. After that, the powdered samples were put in a standard sample holder. XRD analyses were conducted with Cu-radiation at 60 kV and 60 mA, utilizing a graphite monochromator to enhance the precision of the measurements. Diffraction scans were performed over a range in 2-theta of 20–50◦ at a rate of 2◦/min.

3.5 Physical and Mechanical Properties

The physical and mechanical properties of the brick samples were investigated. Physical characterization included measurements of water absorption, porosity, and the saturation factor. The mechanical assessment involved determining the bulk density, breaking load, and compressive strength.

3.6 Measurement of Water Absorption Rate

This section delineates the experimental procedure employed for the quantification of the water absorption rate in the brick and rock specimens under investigation, as follows [13-15] :

The requisite apparatus for conducting the test comprised a ventilated oven, certified to maintain a uniform and stable temperature regime of 110–115°C. Mass measurements were conducted using an analytical weighing balance possessing a minimum capacity of 2000 g and a precision of ±0.5 g. Specimen immersion was facilitated by a tank of sufficient dimensions to allow for the complete submersion of individual bricks in water. The immersion medium consisted of clean, potable water maintained at ambient room temperature. Finally, a damp, absorbent cloth was utilized for the meticulous removal of superficial water from the saturated specimens before weighing.

i) Selection and Preparation

A representative sample of two intact bricks was randomly selected from the batch to ensure statistical significance. All specimens were visually inspected and confirmed to be free of defects, including cracks and chips, which could compromise the integrity of the test results. The selected bricks and rocks were subjected to a drying process in a ventilated oven stabilized at a temperature of 110 ± 5°C. Drying continued until a constant mass was achieved, a condition defined as a mass loss of no more than 0.2% between two successive weighing conducted at two-hour intervals. Upon reaching constant mass, the specimens were transferred to a desiccator and allowed to cool to ambient temperature to prevent atmospheric moisture absorption prior to initial weighing.

ii) Test Procedure

The cooled mass of each specimen was recorded as its dry weight. Subsequently, the bricks or rocks were completely immersed in a tank of potable water maintained at 27 ± 2°C for a duration of 24 hrs, ensuring full submersion at all times. Following the immersion period, each specimen was promptly removed from the water. Any excess surface moisture was meticulously blotted using a damp, lint-free cloth, and the saturated weight was determined within 3 min of removal to minimize error due to water evaporation.

The water absorption capacity for each individual specimen was calculated as a percentage of its dry mass according to the formula [16]:

$$\text{Water Absorption (\%)} = [(Ws - Wd) / Wd] \times 100$$

Where,

Ws = the saturated weight in grams

Wd = the dry weight in grams

The final reported water absorption value for the batch is the arithmetic means of the results obtained from the two individual specimens.

iii) Measurement of porosity (%) in bricks

The procedure for measuring porosity using the gravimetric method is a multi-step process that requires careful control of variables to ensure accuracy [17].

iv) Sample preparation and drying

The first step is to prepare the brick and rock samples. While full-size samples were typically used for standardized testing, some research suggests that using representative 20-mm crushed lumps is more effective for removing trapped air and achieving saturation. Regardless of the sample size, the specimens were cleaned of any foreign materials, like dirt or mortar. They were then dried in a ventilated oven at a temperature of 105 to 115°C until they reached a constant mass, which was recorded as the dry mass (Wd). The process of drying to a constant mass ensured that all absorbed moisture had been removed from the specimen before testing began.

v) Saturation via water immersion

Upon achieving a constant dry mass, the specimens undergo a saturation process. This was accomplished through several established methods. Cold immersion involves fully submerging the dried bricks in water maintained at a controlled temperature of approximately 27°C for a minimum duration of 24 hours, a process that relies on capillary action for water ingress. For a more rigorous and complete saturation, as often mandated by standards such as ASTM C67, the boiling immersion method was employed. This technique required submerging the specimens in boiling water for a period of 5 hrs; the boiling process was conducted to expel trapped air from the pore network, thereby enabling water to penetrate a greater volume of the open voids. In addition, immersion was also accomplished by a vacuum before immersion, which actively evacuated air from the internal pore structure and allowed water to subsequently fill nearly all accessible voids.

vi) Measuring key masses

After the saturation was completed, the specimens were removed from the water, and then their surfaces were quickly wiped to a saturated-surface-dry condition, and their mass (Wssd) was recorded within 3 min of removal to prevent evaporation. The specimens were then weighed while fully submerged in water. This submerged mass (Ws) was a critical value for calculating the displaced volume of the specimen.

The porosity rate was derived from the measured mass values. The formula for apparent porosity (Pa) was derived from the dry mass, saturated-surface-dry mass, and submerged mass. The apparent porosity, which measured only the interconnected pore volume, was calculated as follows [18]:

$$\mathbf{Pa} = \frac{\mathbf{Wssd - Wd}}{\mathbf{Wssd - Ws}} \times \mathbf{100\%}$$

Here, Wssd−Wd represents the mass of water absorbed, which is equivalent to the volume of the open pores, and Wssd−Ws represents the volume of the bulk sample (mass of displaced water).

The saturation coefficient is another important metric derived from this method, calculated by dividing the absorption value from the 24 hrs cold immersion by the absorption from the 5 hrs boiling immersion.

vii) Measurement of Saturation Coefficient in Bricks

The saturation coefficient was determined for the brick and rock specimens to assess their potential durability, specifically their resistance to damage from freeze-thaw cycles. This coefficient, also known as the C/B ratio, is a critical parameter defined in standards such as ASTM C67. It represents the ratio of water absorbed by a sample under simple immersion (cold water) to that absorbed after a more rigorous saturation process (boiling). A lower saturation coefficient suggests a greater volume of unfilled pores is available to accommodate the expansion of water upon freezing, thereby enhancing the brick or rock's frost resistance [19-21].

The experimental procedure began with the preparation of a representative sample of at least five full-size specimens. These specimens were first dried in a ventilated oven at a controlled temperature of 110-115°C. The drying process continued until each specimen reached a constant mass, which was confirmed when the mass difference between two consecutive weightings, taken at two-hour intervals, was negligible (less than 0.2% of the total mass). After drying, the specimens were allowed to cool to room temperature in a desiccator to prevent moisture reabsorption. The constant mass of each cooled specimen was then accurately recorded as its dry weight (Wd).

The measurement process involved a two-stage water absorption test performed sequentially on the same specimens. In the first stage, the dry, weighed specimens were fully submerged in a tank of clean water maintained at room temperature (24 ± 8°C) for 24 hrs to allow the natural absorption of water into the easily accessible pores. After the 24 hrs immersion, each specimen was removed from the water, its surface was carefully wiped with a damp cloth to remove excess water, and it was immediately weighed. This mass was recorded as the saturated weight after cold immersion (Wc).

In the second stage, the same specimens were returned to the immersion tank and submerged again. The water was then heated to its boiling point and maintained at a boil for 5 hrs. This boiling process is designed to expel trapped air from the finer pores and achieve a state of near-complete saturation. Following the boiling period, the specimens were left to cool to room temperature while remaining fully submerged to prevent air from re-entering the pore network. Once cooled, each specimen was removed, its surface was wiped with a damp cloth, and it was weighed immediately to determine its saturated weight after boiling (Wb). This value represents the total water absorption capacity of the brick's open-pore system.

The saturation coefficient (S) was then calculated for each specimen using the three measured weights. The calculation is based on the ratio of the mass of water absorbed during the 24-hour cold soak to the mass of water absorbed during the 5 hrs boil. The formula used was as follows:

$$\text{Saturation Coefficient (S)} = (Wc - Wd) / (Wb - Wd)$$

The numerator (Wc - Wd) represents the water absorbed by cold immersion, while the denominator (Wb - Wd) represents the water absorbed by boiling. The final saturation coefficient was reported as the average of the values obtained from the sample set, providing a reliable index of the material's frost durability.

3.7 Mechanical properties

The mechanical properties of the bricks were determined for samples collected from different sites in TO, as illustrated in Fig.6, to illustrate the difference in mechanical properties as the variation in site, and therefore the weather conditions, affects the durability of the tested bricks.

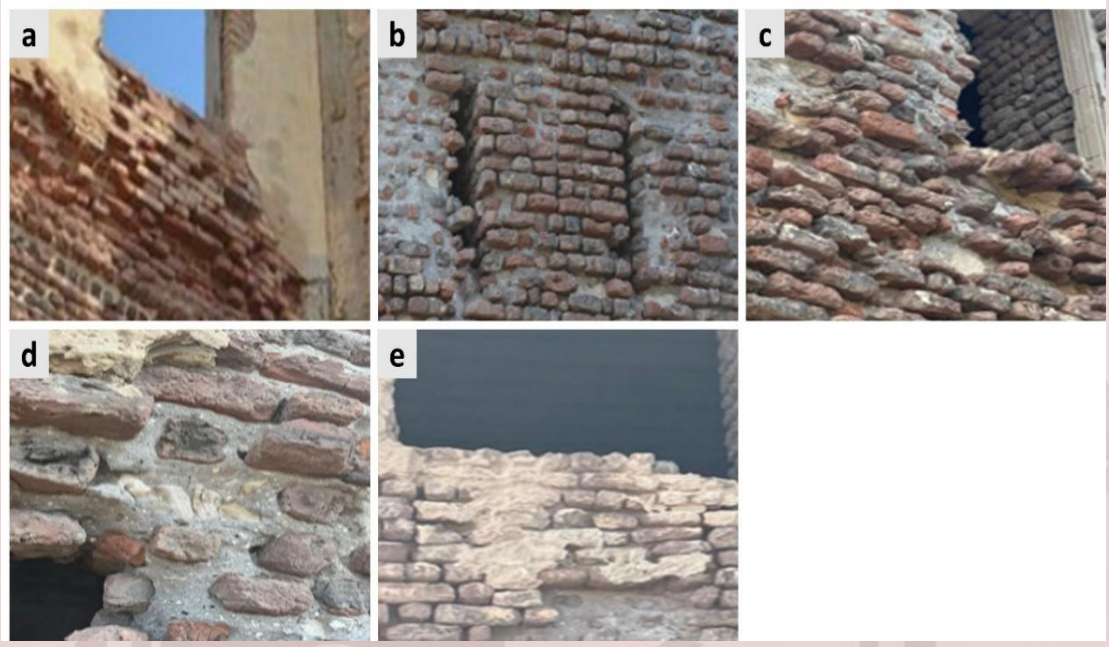

Fig. 6. Figure s for brick sites of a) first, b) second, c) third, d) fourth, and e) fifth sites, respectively.

i) Measurement of Bulk Density in Bricks

The bulk density of the brick specimens was determined to provide a key measure of the material's compaction and weight per unit volume. The methodology employed is based on the principles of Archimedes and is consistent with the procedures outlined in established standards such as ASTM C20-00(2015). This method involves measuring the dry mass of the brick and its exterior volume, which is determined by the volume of water it displaces [22].

Initially, a representative sample of at least three whole brick specimens was selected for the analysis. To ensure that the measured mass was solely that of the solid material and not influenced by moisture content, the specimens were first dried to a constant mass. This was achieved by placing them in a ventilated oven maintained at a uniform temperature of 110-115°C. The specimens were weighed at 2 hrs intervals, and the drying process was considered complete when the mass variation between consecutive weightings was less than 0.1% of the specimen's total mass. After reaching a constant state, the bricks were allowed to cool to room temperature in a desiccator to prevent the reabsorption of atmospheric moisture. The mass of each cooled, dry specimen was then accurately measured and recorded as the dry weight (Wd).

Following the determination of the dry weight, the exterior volume of each specimen was measured using the water displacement method. This required the complete saturation of the specimen's open pores to prevent water from

infiltrating during the volume measurement. Saturation was achieved by submerging the specimens in a tank of distilled water and boiling them for a minimum of 5 hrs. After the boiling period, the specimens were left to cool to room temperature while remaining fully submerged in the water.

Once cooled, the mass of each saturated specimen was determined under two distinct conditions. First, the specimen was weighed while fully suspended in water using a harness or basket. This measurement, recorded as the suspended weight (Wsusp), is crucial for determining the specimen's volume based on Archimedes' principle. Subsequently, each specimen was removed from the water, its surface was quickly patted dry with a damp cloth to remove excess water, and it was immediately weighed in air. This mass was recorded as the saturated weight (Wsat). The exterior volume (V) of the specimen was calculated from the difference between its saturated and suspended weights, as this difference is equal to the mass of the displaced water.

The bulk density (ρb) was then calculated for each specimen using the following formula:

$$\text{Bulk Density } (\rho b) = Wd / (Wsat - Wsusp)$$

Where,

Wd = the dry weight of the specimen

The denominator (Wsat - Wsusp) = the exterior volume of the specimen in cubic centimeters (assuming the density of water is 1 g/cm³).

ii) Measurement of Breaking Load and Compressive Strength

- **Breaking Load**

The measurement of breaking load in bricks is a key indicator of their mechanical strength and durability. The term "breaking load" typically refers to two distinct types of tests: **compressive strength** and **flexural strength** (or Modulus of Rupture). Both methodologies are standardized and are commonly detailed in technical specifications like **ASTM C67** [23-25].

This test measures a brick's ability to resist forces that try to crush it. It's the most common and important test for determining a brick's overall load-bearing capacity. A minimum of five whole bricks is dried in a ventilated oven to a constant weight at a temperature between 105 °C and 115 °C. For an accurate test, the two bearing surfaces (the faces that will be in contact with the testing machine) must be smooth and parallel. If the surfaces are not naturally flat, they are "capped" with a thin, smooth layer of a high-strength material like sulfur-gypsum mortar or Portland cement paste.

The prepared brick specimen is placed in a **universal testing machine**. The specimen is carefully centered to ensure the load is applied evenly. A continuous, uniform load is applied to the brick at a specified rate (e.g., between 1,000 to 2,000 lbf/min or 4.4 to 8.9 kN/min) until the brick fails. The maximum load at which the brick breaks is recorded. The compressive strength is calculated by dividing the maximum load by the gross cross-sectional area of the brick.

Compressive Strength=Gross Cross- Sectional AreaMaximum Load at Failure

The result is typically expressed in units of megapascals (MPa) or pounds per square inch (psi).

- Flexural Strength Methodology (Modulus of Rupture)

This test measures the brick's ability to resist bending forces, which is important for applications like paving or lintels where the brick may experience stress from its center. As with the compressive strength test, five whole bricks are dried. The length, width, and depth of each brick are measured to the nearest 0.1 inch or 2.5 mm.

The brick is placed on two rounded supports spaced a specific distance apart (typically 7 inches or 178 mm) on the bed of the testing machine. The load is then applied to the top center of the brick, at a uniform rate, until the brick breaks. The maximum load is recorded. The flexural strength, or Modulus of Rupture (MR), is calculated using the following formula:

$$MR=2bd23PL$$

Where: P = Maximum load recorded at failure, L = Span between the supports, b = Average width of the brick, and d = Average depth of the brick

The result is also expressed in MPa or psi. This test is often performed first, and the resulting broken halves of the brick can then be used as specimens for the compressive strength test.

3.8 Total Bacterial Count

The total bacterial count in the examined samples was measured using the plate count method. Serial decimal dilutions were prepared and shaken thoroughly. One milliliter of the last three dilutions was transferred to Petri dishes in triplicate. Subsequently, 15 ml of nutrient agar medium was added, and the mixture was incubated at 37 °C for 72 h. The developed colonies were counted [26-30].

Bacterial Identification

Three different bacterial colony morphologies were obtained during the experiment to determine total bacterial count, isolate the colonies with different morphologies, and identify them based on their culture characteristics, cell morphology, arrangement, and the use of selective media, according to the method described by [31].

3.9 Statistical analysis

The results obtained from different tests were statistically analyzed using the Costat program version 6.311 (CoHort software, Monterey, USA). The tested samples were compared using statistical analysis of variance (ANOVA). Moreover, the standard deviation (SD) of the obtained data was calculated. Duncan's new range test at P = 0.05 was used to determine significant variations among all means. Each sample in this study was analyzed three times [32-34].

4. Results and discussions

The detailed study for the investigation and characterization of the construction materials, including wood, bricks, stones, and mortars in TO of Egypt, is illustrated hereunder.

4.1 Morphology and color analysis of the bricks by visual observation

The morphology and color of the tested samples of bricks, mortar, stone, and wood were visually observed, as illustrated in Table 1. The tested bricks exhibited irregular edges, surfaces, and textures. The main texture is fired clay, which was hand-molded and then fired. Their color ranged from reddish-brown to black, which may be due to the ratio of firing, with darker scattered areas corresponding to different firing temperatures. The brick contained low-mineral air pockets, as observed in the tested brick samples. In addition, stone cutting showed clear evidence of manual cutting, and the texture and white powder revealed that the tested stone was limestone with a color ranging from off-white to light grey.

The mortar used to bind the observed bricks and stones were a combination of sand and fine aggregates. The remaining compositions were difficult to analyze visually and required further chemical analyses for identification. The tested mortar was off-white to dark gray in color. Wood samples were likely used as beams to resist high moments at mid-spans and as structural support. The grain pattern and visible tool marks revealed that the object was not manually shaped using cutting machines. Their surfaces showed signs of age-related degradation, but there were many marks for white paint; however, there were some cracks at the lower parts of the wood due to long-term exposure to heat and moisture. Other samples included many holes, as evidence of containing wild ants. Moreover, most wood samples showed light yellow to dark yellow coloration.

4.2 Microstructural degradation analysis via scanning electron microscopy (SEM)

SEM analysis was conducted to characterize the microstructural features indicative of degradation and to correlate these observations with the effects of weathering and erosion. The primary observations and inferred degradation mechanisms for the samples studied were discussed in this study, as follows:

Fig. 7a and b show severe degradation of the surfaces of wood samples, characterized by fractured cell walls, fiber separation, and voids, indicating advanced biological decay. This is consistent with fungal (brown, white, and soft rot) and bacterial activity, which causes distinct microstructural changes, such as cellulose and hemicellulose degradation or complete cell wall breakdown [35-38]. Moreover, the surfaces of the brick samples displayed in **Fig.7c and d** reveal erosion, high porosity, microcracks, and granular disaggregation. These features are primarily caused by salt crystallization, thermal stress, and freeze-thaw cycles [39-40].

Salt crystallization exerts expansive pressures, thermal stress causes differential expansion and microcracking, and freeze-thaw cycles lead to hydraulic pressure damage, all of which are exacerbated by brick porosity. Additionally, mortar sample surfaces show a porous matrix with microcracks and calcite formations, along with voids at the binder-aggregate interfaces in **Fig. 7e and f**. Degradation is driven by carbonation, salt crystallization, and freeze-thaw cycles [42-43]. Carbonation alters the pore structure, salt crystallization creates internal stresses, and freeze-thaw cycles cause progressive disintegration, all of which contribute to microstructural deterioration.

Finally, the rock samples, which are displayed in **Fig. 7g and h,** have a granular, uneven surface with loosened, 'sugar-like' grains and inter/intra-crystalline microfractures. This indicates significant physical and chemical weathering, predominantly thermal stress weathering [44-45]. The differential thermal expansion of minerals creates internal stresses, leading to microfractures and granular disaggregation, which in turn increases susceptibility to chemical leaching and biological activity.

SEM analysis confirmed advanced and systemic degradation across all examined materials (wood, brick, mortar, rock) from the historical TO. The deterioration may be due to a complex interplay of physical, chemical, and biological processes, which are exacerbated by long-term environmental exposure. Widespread microcracking, granular disintegration, and biological activity pose a significant threat to the structural integrity of the TO and must be considered in future conservation strategies.

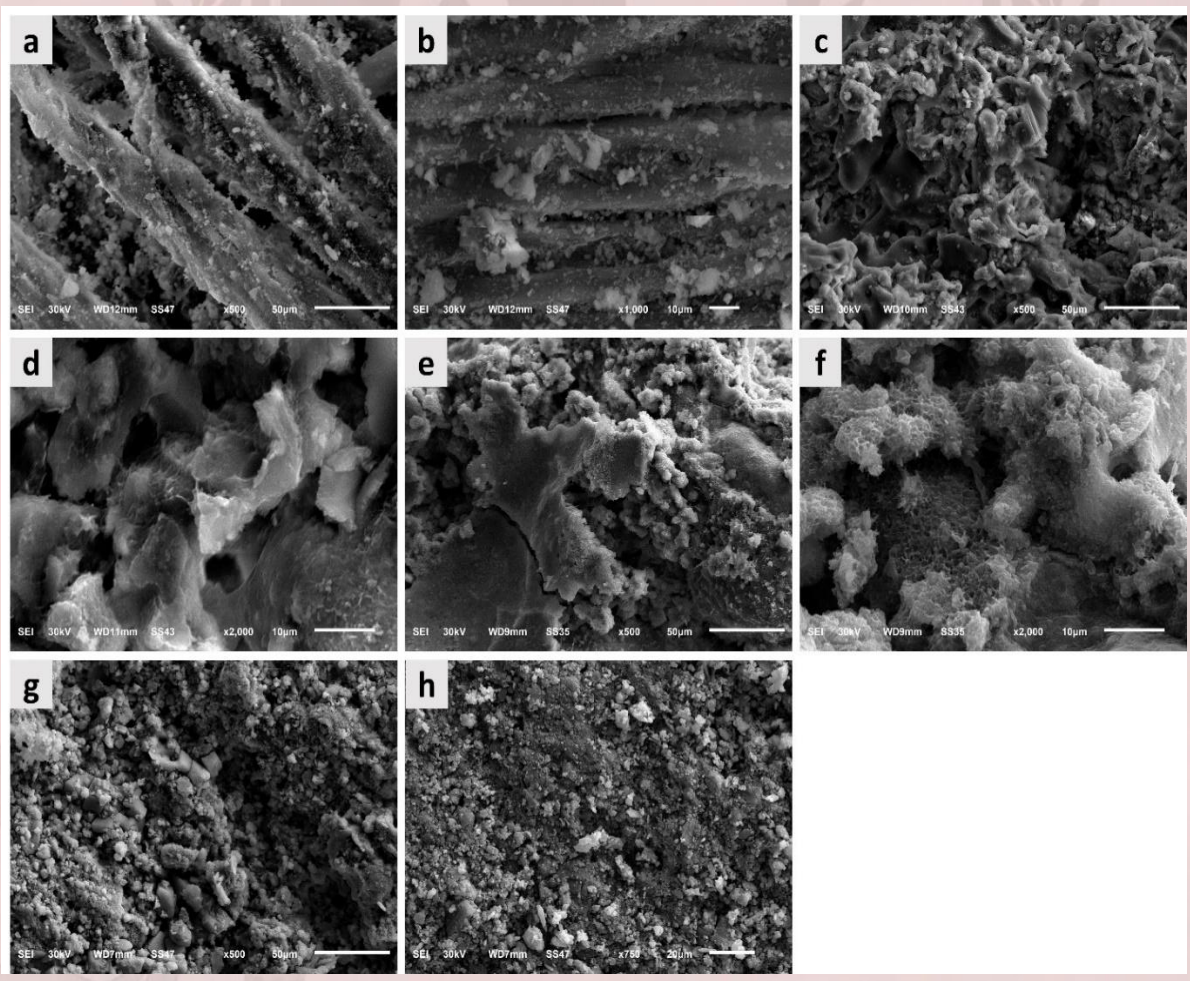

Fig. 7. SEM micrograph of the tested samples' surfaces of a,b) wood, c,d) bricks, e,f) mortar, and g,h) rocks.

4.3 EDX analysis

EDX analysis provides useful screening information; confirmatory phase and ion analyses are recommended before conservation interventions. In this respect, EDX analysis of wood surfaces showed low-energy C and O peaks corresponding to lignocellulosic substrates [46]. These peaks of various exogenous minerals are superimposed on them, showing sodium, magnesium, aluminum, silicon, sulfur, chlorine, potassium, calcium, and trace iron or titanium [47]. Based on EDX analysis, the minerals may not have been part of the wood but were deposited on it. The Na and Cl both point to sodium chloride, which may be halite from sea sprays or aerosols. At the same time, the magnesium with Cl and S suggests magnesian salts like magnesium chloride or magnesium sulfate [48]. In addition, the peaks of Si, Al, and K show siliceous dust or silicate clays or feldspars. The calcium in the presence of sulfur indicates fine calcite or gypsum, picked mortar. Therefore, the surfaces of wood need to be cleaned well before the potential conservation process.

Fig. 8 (b) shows the EDX analysis of bricks, which illustrates that high Si and Al levels are characteristic of silicates (in this case, clay) and form the framework mineralogy of the bulk alumino silicate of the bricks. Furthermore, the high content of Fe may correspond to iron oxides present in the red and brown fired clays. In addition, the detectable Ca is due to lime source of bricks, and mortar attached to the brick's surface. Moreover, the common trace minerals of the natural clays, such as Ti, Mg, and K, were observed in EDX analysis of the tested brick samples. Na and Cl peaks may indicate the presence of salts on the surface of bricks as a result of weather conditions.

Regarding mortar samples, they showed a strong presence of Ca, suggesting mortar based mostly on lime (Portland/lime/secondary calcite) with surface cross-cement based on the limiter functional for historical mortars used. The co-existence of Si and Al in the mortar suggests there is sand (silica and aluminosilicates) added. Cl and Na on the surface of the mortar suggest contamination from soluble salts (marine aerosols).

Additionally, the large peak in calcium, along with modest silicon content and presence of oxygen, relates most closely to a limestone or calcite-rich stone. The presence of silicon, aluminum, and magnesium in very low concentrations is characteristic of accessory silicate minerals or sand inclusions. The chloride and sodium ions also indicate salt deposition on the surface of the rock, like bricks and mortar.

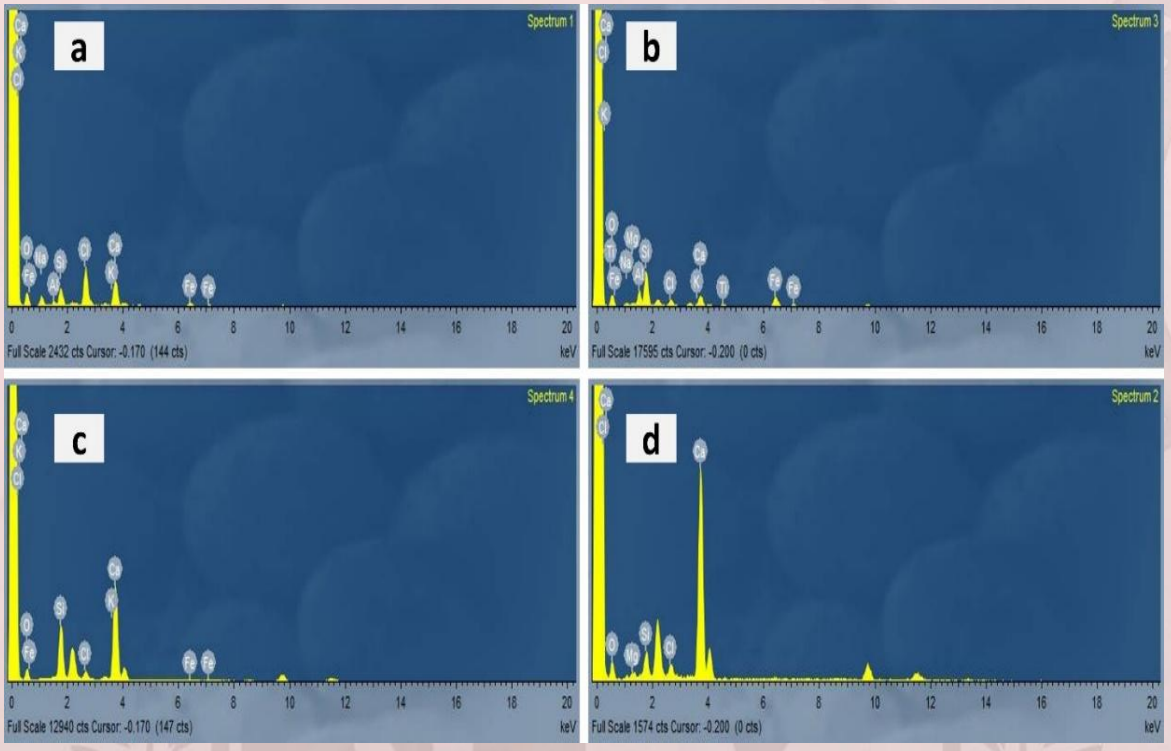

Fig. 8. EDX analyses the tested samples' surfaces of a) wood, b) bricks, c) mortar, and d) rocks.

4.4 XRD Analysis

The XRD pattern of the brick sample shows that the phases of sodium calcium aluminum silicate are the most prominent, although there are small amounts of silicon dioxide. This type of mineralogy is known for fired clay ceramics rich in feldspathic and silicate phases, which is indicative of brick making in Egypt. Even small amounts of crystalline silica indicate that the raw material was quartz sediment rich. While these phases aid in the brick's mechanical strength and overall durability, an excess of quartz can cause microcracking due to thermal expansion mismatches during firing.

In addition, the rock samples primarily consist of dolomite, magnesium, calcium carbonate, and calcite, calcium carbonate. This further supports that the raw stone material used for the construction of TO was quarried in Egypt from stone sites rich in carbonate. When compared to pure limestone, dolomite-rich stones are more durable against weathering due to the higher composition of weathering-resistant minerals.

The internal mortar sample is entirely composed of calcium sulfate hydrate (gypsum). This finding confirms the use of gypsum plaster as a binding material, a practice historically documented in Egypt due to the abundance of natural gypsum deposits. Gypsum mortars offer advantages such as rapid setting and good adhesion; however, they are highly soluble and vulnerable to moisture infiltration, which can cause volumetric changes, powdering, and eventual loss of cohesion. On the other hand, the external mortar displays a dominance of silicon oxide (quartz) and a notable fraction of calcium carbonate. This mixture implies the use of sandy aggregates bound with a lime-based matrix. Such lime-silica mortars are characteristic of traditional construction techniques, offering enhanced durability, breathability, and resistance to weathering compared to gypsum-based mortars.

The tested samples indicated an intentional separation of construction materials depending on their functional purposes. In order to achieve structural strength, bricks were made of silicate-rich compositions, while local carbonate rocks served as structural blocks. There were different types of mortar; gypsum mortars were used solely for internal applications, while external applications for silicate-lime mortars were to increase weathering resistance. This arrangement confirms Egyptian knowledge of advanced materials for construction and the ability to provide balance among availability, function, and robustness of building materials [49-50].

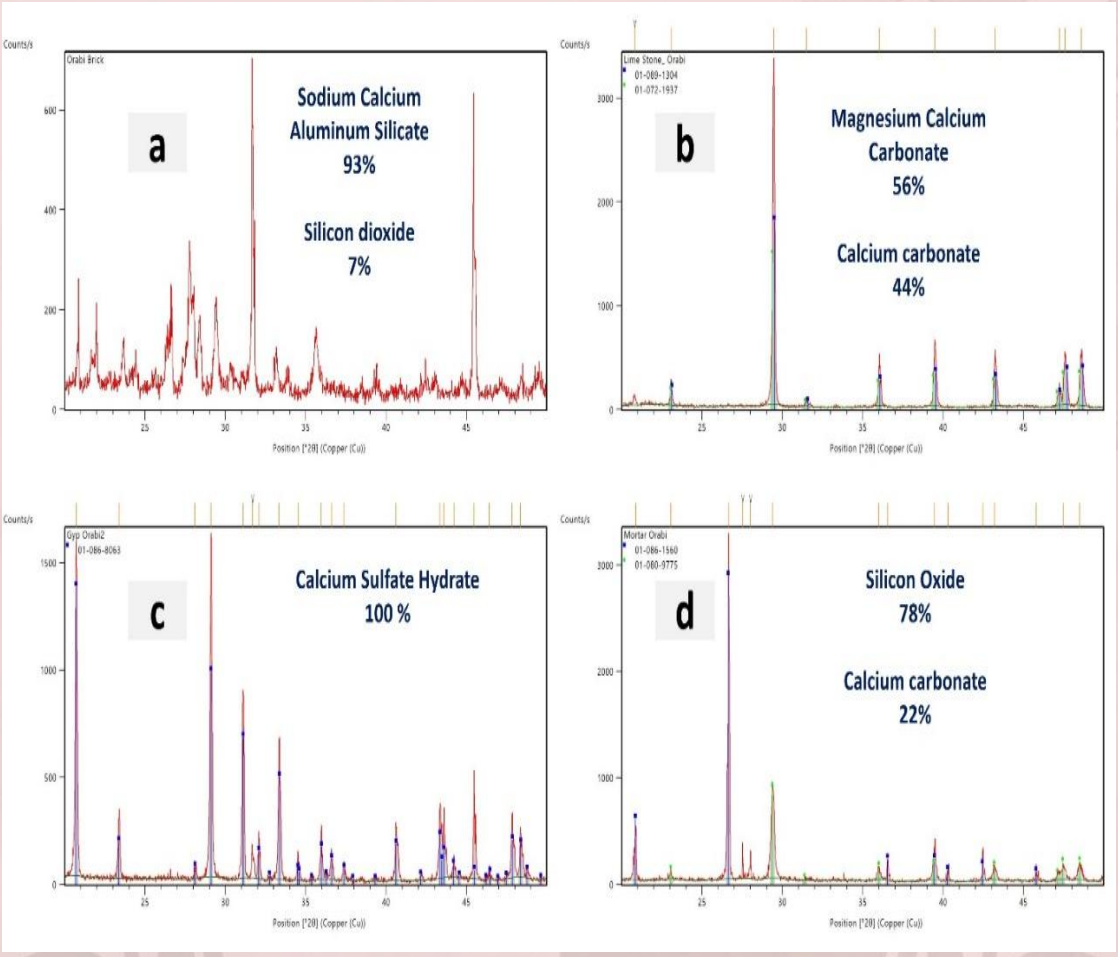

Fig. 9. XRD patterns of a) bricks, b) rocks, c) internal mortar, and d) external mortar

4. 5 Engineering Properties

i)Physical properties of bricks and rocks

The statistical analysis of the physical and mechanical properties of the samples reveals significant variations among the tested brick and rock samples obtained from TO, with notable variations observed not only between the bricks and rocks but also among the brick samples themselves. These findings are crucial for understanding the suitability and durability of these materials in their respective applications.

The descriptive statistics for the physical properties of the brick and rock samples are presented in Table 4.1 These properties include absorption rate, porosity rate, and saturation factor. From the analysis, it was observed that brick samples have a higher mean absorption rate (11.81%) compared to rock samples (5.10%). This higher absorption rate in bricks makes them more susceptible to freeze-thaw damage and chemical weathering, particularly in environments with high

humidity or frequent temperature fluctuations. Conversely, rock samples exhibit a slightly higher mean porosity rate (15.77%) than brick samples (12.91%).

This indicates differences in pore structure and connectivity. The saturation factor for rock samples (1.10) is also higher than that for brick samples (0.89), which indicate their capacity to hold water relative to their pore volume. A higher saturation factor is critical, as exceeding a certain degree of saturation can lead to freeze-thaw damage. The results obtained showed that bricks, in general, based on their physical properties, were more susceptible to degradation and deterioration than rocks, and therefore they have been periodically in need of conservation process.

STARDOM UNIVERSITY

Table .1. Physical properties for bricks and rocks

Samples	Absorption rate (%)	Porosity rate (%)	Saturation Factor
Bricks	11.8 ± 1.625 a	12.91 ± 3.800 a	0.89 ± 0.051 b
Rocks	5.10 ± 0.260 b	15.77 ± 1.124 a	1.10 ±0.055 a

ii) Mechanical properties of the tested bricks

Table (2) displays the descriptive statistics for the mechanical properties of brick samples obtained from different sites. These properties, which include bulk density, breaking load, and pressure resistance, reveal considerable variation, which is attributed to differences in raw materials, firing temperatures, and manufacturing processes. Site 2 exhibits the highest mean breaking load (13754.67 N) and pressure resistance (5.24 N/mm²), which are both statistically significant ($p<0.05$) compared to the other sites. This suggests that the bricks from Site 2 possess superior structural integrity and are more resistant to compressive forces. The stress-strain curves **(Fig. 10a-e)** corroborate this, with the curve for Site 2 **(Fig. 10b)** showing a steeper initial slope and a higher peak stress, indicative of a more rigid and stronger material.

Conversely, the bricks from Site 1 show the lowest mean breaking load (4780.67 N) and pressure resistance (2.20 N/mm²), indicating a weaker material. The stress-strain curve for Site 1 **(Fig. 10a)** has a lower peak and a more gradual failure, which is consistent with its lower strength values. The mechanical properties of samples from Sites 3, 4, and 5 fall between these two extremes, with some overlapping statistical significance. The bulk density of the brick samples ranges from a mean of 1.26±0.075 g/cm^3 for samples from Site 3 to 1.48±0.089 g/cm^3 for samples from Site 2. The variations in bulk density among different sites for bricks suggest differences in their composition. Generally,

higher bulk density correlates with higher strength and durability in building materials.

Overall, the observed differences in mechanical behavior indicate that the preservation state of the bricks is site-dependent. Environmental exposure, construction techniques, and historical repair interventions are likely the key factors influencing these variations. These findings underline the importance of site-specific conservation strategies to ensure the structural stability and long-term preservation of Tabia Oraby.

Table .2. Mechanical Properties for Brick Samples from Different Sites

Bricks sample sites	Bulk Density (g/cm^3)	Breaking Load (N)	Pressure resistance (N/mm^2)
First site	1.32 ± 0.065 ab	4780.67 ± 619.681 d	2.20 ± 0.479 c
Second site	1.48 ± 0.089 a	13754.67 ± 1242.097 a	5.24 ± 0.811 a
Third site	1.26 ± 0.075 b	9458.67 ± 1113.633 b	4.33 ± 0.401 ab
Fourth site	1.38 ± 0.146 ab	7002.33 ± 974.281 c	3.18 ± 0.752 bc
Fifth site	1.40 ± 0.106 ab	10829.67 ± 1047.531 b	5.23 ± 1.035 a

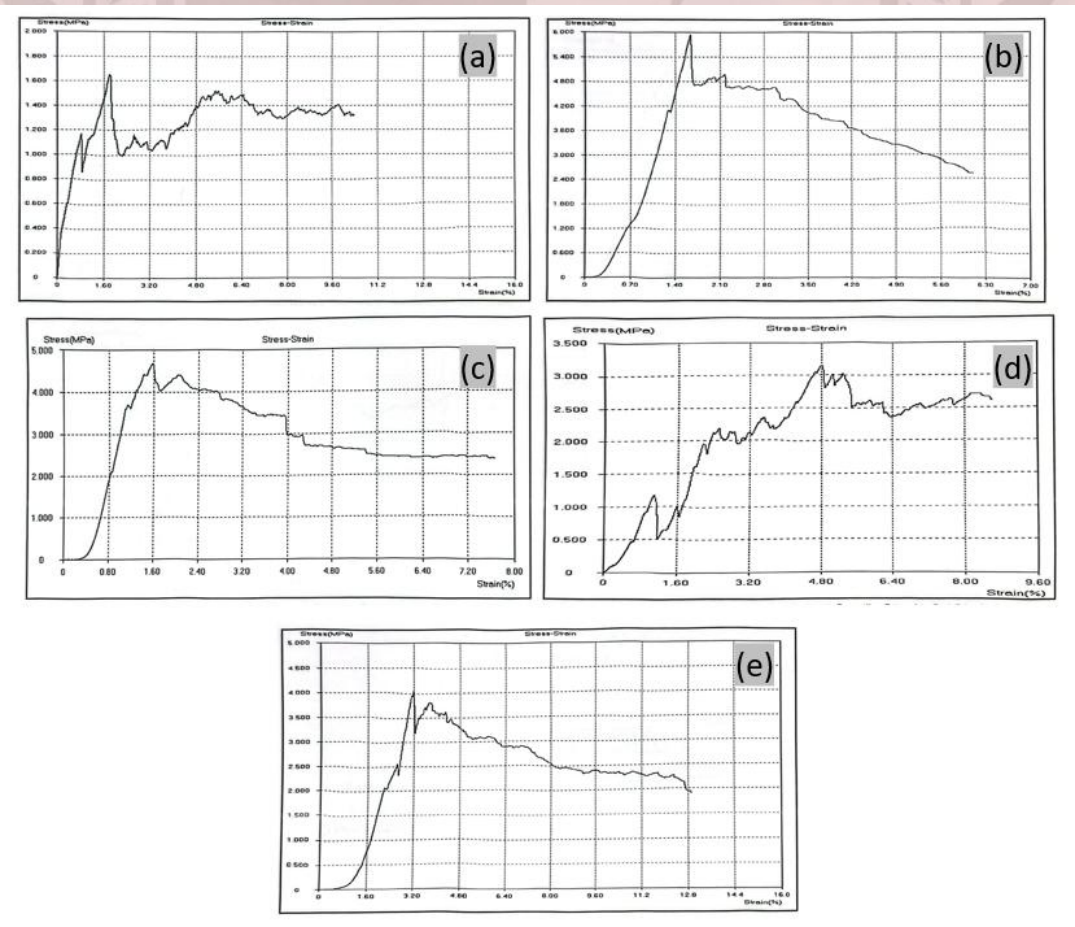

Fig. 10. Uniaxial compressive stress-strain curves for brick samples from Sites a) first, b) second, c) third, d) fourth, and e) fifth sites, respectively.

4.6 Microbiological Examination

i) Total bacterial count

Table (3) displays the total number of bacteria found on our different building materials. According to the data, there are notable differences in the microbial colonization of various materials, with stone showing the lowest bacterial load and wood the highest.

Table. 3. The total bacterial count of the tested construction samples of TO

Construction samples	Total bacterial count
Wood	81 ± 2.8 a
Brick	56 ± 1.8 b
Mortar	45 ± 1.4 c
Rock	19 ± 1.1 d

Bacterial loads varied across the sampled material classes (wood, bricks, mortar, and stone) owing to differences in the physical and chemical properties of the materials. Wood, being an organic material, can provide a carbon and nutrient source to support bacterial growth. Wood is also porous, with a large surface area that absorbs moisture and provides an ideal microenvironment for the establishment of a microbial community. The highest number of bacteria on wood (81 ± 2.8 CFU/g) correlates with the established knowledge that wood is a highly biodegradable material owing to the effects of several wood-decaying bacteria and fungi. [51-55].

Bricks and mortar are generally inorganic materials but may contain organic impurities and often exhibit porous structures that can absorb moisture. The bacterial counts found on bricks (56 ± 1.8 CFU/g) and mortar (45 ± 1.4 CFU/g) were lower than those on wood but were still significant enough to suggest an ability to establish significant microbial populations. Microorganisms can penetrate these materials over time, exposing them to degradation of these materials to discoloration, degradation of the structural integrity of bricks and mortar, release of corrosive metabolites such as nitric acid from nitrifying bacteria, and, in the case of carbonated structures, the subsequent complete loss of structural integrity. [56-59].

Rock, especially dense versions, had the lowest bacterial count (19 ± 1.1 CFU/g), largely due to its very low proportion and less organic material than other materials, let alone previous items. However, stone monuments are not free from microbial attacks. Microorganisms establish biofilms on stone surfaces, and their metabolic activities associated with these microorganisms can create both physical and chemical changes, including bioprinting, dissolution of minerals, and even the formation of secondary minerals. Cyanobacteria and algae can colonize stone surfaces and distract visually, while retaining moisture that could enhance other bacteria and/or fungi.

Historical monuments located in the open air allow for constant invasion by microbes, and environmental conditions combined with pollutant types provide a continuum and multiple types of colonization by microbes. Biofilms, a group of microorganisms in an extracellular polymeric substance, are an important part of bio deterioration, having the capacity to protect other microbes in a biofilm, tolerate environmental conditions, and take in nutrients that locally damage the monument.

These results highlight the urgent need for conservation strategies designed to manage microbial biodeterioration. Periodic inspections of microbial loads of various materials can provide updates on the monument's condition and alert the conservator to intervene when appropriate. Bio conservation techniques, which employ environmentally neutral methods to impede the growth of microbial populations on monuments, or bioclimatic techniques, are increasing in popularity. This includes the application of antimicrobial materials, the selective use of biocides on targeted organisms, or the modification of environmental conditions to inhibit their growth. Knowledge of the community composition and ecology of applicable microbial communities with respect to material resources of the bio cultural heritage site is essential for developing unique, sustainable conservation regimes for historic monuments.

iii) Bacterial identification

The first isolate was white and round on the agar surface, and the cells were short rods, arranged singly. When grown on selective media, it formed colonies with a metallic sheen on the EMB medium. Based on these characteristics, the isolates are identified as E. coli. This genus was widespread in all samples as shown in **Table (4) and Fig.11** (a-c)**.** The second isolation was circular colonies under the surface of the medium, and its cells were long, rod-shaped, and spore-laden with a terminal spore. When it was grown on a cooked meat medium and covered with a layer of Vaspar, a rise in Vaspar was observed above the surface of the medium after 24 hours. Based on these characteristics, the isolates are identified as

Clostridium sp. This genus was present only in sample 2, as shown in **Table (4) and Fig. 12(d-f).** The third isolate has a large white colony with serrated edges and long rod-shaped cells. Based on these characteristics, the isolates are identified as Bacillus sp. This genus was widespread in all samples, as shown in **Table (4) and Fig.13.**

Table. 4. The identified bacterial strains in the construction materials obtained from TO

Bacterial strain	Brick	Wood	Rocks	Mortar
E. coli	√	√	√	√
Clostridium sp.	x	√	x	x
Bacillus sp.	√	√	√	√

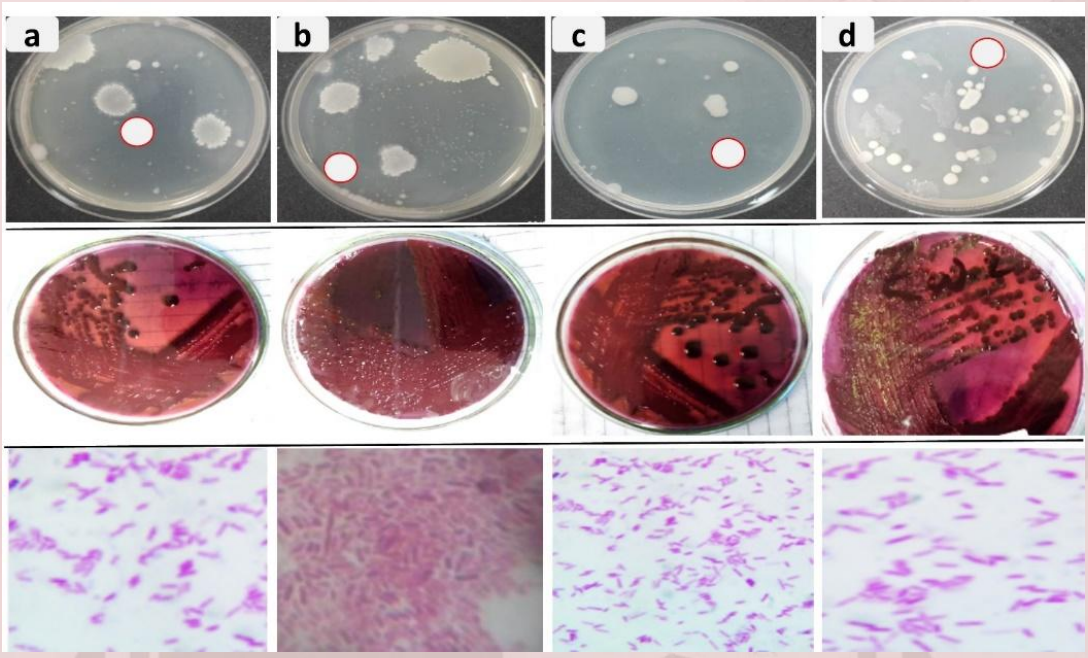

Fig. 11. Identification of E. Coli isolated from a) brick, b) wood, c) rock, and d) mortar.

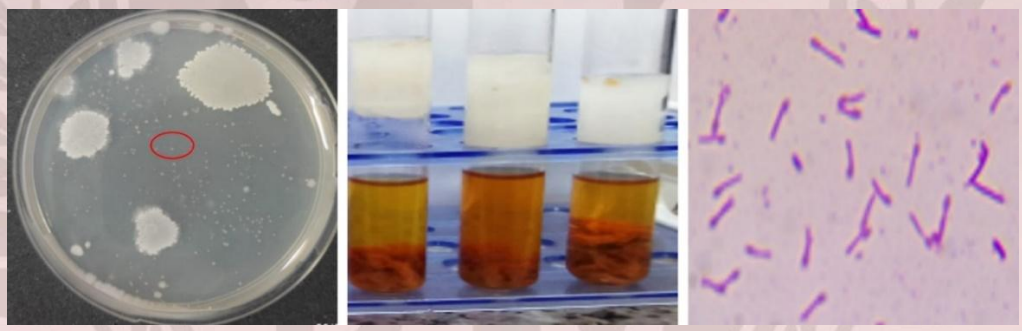

Fig. 12. Identification of Clostridium sp. isolated from a) brick, b) wood, c) rock, and d) mortar.

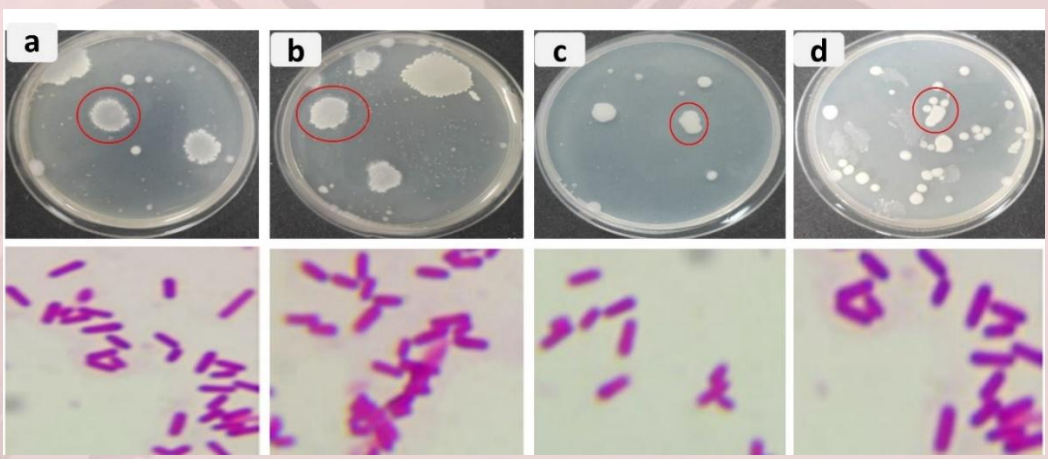

Fig. 13. Identification of Bacillus sp. isolated from a) brick, b) wood, c) rock, and d) mortar.

Conclusion

Several chemical, physical, mechanical, and microbial investigations were conducted on the construction materials used in Tabia Oraby (TO) buildings. In this respect, the morphology of the surfaces of the construction materials was examined using SEM analysis, which showed an obvious deterioration due to exposure to different biological, physical, and chemical factors. The chemical composition was determined using XRD and EDX analyses to select the best materials for the conversion process in advance.

Additionally, physical tests conducted on bricks and rock samples, including absorption rate, porosity rate, and saturation factor, showed that bricks exhibited a higher absorption rate (11.8%) than rocks (5.1%), and lower porosity rate and saturation factor than rock samples. Mechanical properties of rocks obtained from the five different sites showed significant variations in mechanical properties, indicating an obvious deterioration rate based on the brick site. In addition, the total bacterial count of the tested construction materials showed that the wood surface had the highest bacterial count, compared to others, while the rock samples exhibited the lowest bacterial count. Finally, the bacterial identification illustrated the presence of E. coli and Bacillus sp. on the surfaces of all the tested samples, and the presence of Clostridium sp. just on the surfaces of wood, which needs specific treatment to protect it from microbial degradation based on the obtained results.

References

1. Ragheb, G.A. and A. Ragheb, A Multi-Criteria Decision for Touristic Revitalization of Historic Waterfront Based on AHP Analysis: A Case Study of Ezbet El-Borg City, Damietta, Egypt. International Journal of Sustainable Development and Planning, 2021. 16(8): p. 1437-1448.
2. Damietta - Wikipedia.
3. Ancient Egyptian Fortresses - War History. 2018.
4. "The Egyptian Question and the Triple Alliance, 1884-1904" by Calvin Alexander Roberts.
5. COLONIALISM AND REVOLUTION IN THE MIDDLE EAST, BY: Juan R. I. Cole P. 2016.
6. Six Essential Reasons to Save Old Places | National Trust for Historic Preservation.
7. Cultural heritage: 7 successes of UNESCO's preservation work | UNESCO.
8. The Importance of Preserving and Promoting Historic Buildings | Norwalk Tomorrow.
9. Feilden, B., Conservation of historic buildings. 2007: Routledge.
10. Lobovikov-Katz, A., Heritage education for heritage conservation – A teaching approach (contribution of educational codes to study of deterioration of natural building stone in historic monuments). Strain, 2009. 45(5): p. 480-484.
11. Hemeda, S. (2019). Geotechnical and geophysical investigation techniques in Ben Ezra Synagogue in Old Cairo area, Egypt. Herit Sci. Volume 7, Issue 23. https://doi.org/10.1186/s40494-019-0265-y
12. Hemeda, S. (2013) Laser Induced breakdown Spectroscopy and other analytical techniques applied on construction materials at Kom El-Dikka, Alexandria, Egypt. Mediterranean Archaeology and Archaeometry, 13, 103-119.
13. Khalaf, F.M. and A.S. DeVenny, New Tests for Porosity and Water Absorption of Fired Clay Bricks. Journal of Materials in Civil Engineering, 2002.

14. How to Test Water Absorption of bricks.
15. ASTM C67-14 - Standard Test Methods for Sampling and Testing Brick and Structural Clay Tile.
16. Hall, C. and A. Hamilton, Porosity–density relations in stone and brick materials. Materials and Structures, 2015. 48(5): p. 1265-1271.
17. Cultrone, G., E. Sebastián, and M.J. de la Torre, Mineralogical and physical behaviour of solid bricks with additives. Construction and Building Materials, 2005. 19(1): p. 39-48.
Hemeda S. PLAXIS 3D numerical analysis of complex geotechnical problems of colossal built heritage. Herit Sci. 2024;12:32.
18. Hemeda, S. Dynamic characteristics of built heritage using ambient noise recordings. Herit Sci 10, 100 (2022). https://doi.org/10.1186/s40494-022-00730-5
19. Hemeda, S. 3d stability modelling of Tutankhamen,s Tomb (Kv62) using Plaxis 3d with jointed rock model. npj Herit. Sci. 13, 155 (2025). https://doi.org/10.1038/s40494-025-01687-x
20. Hemeda, S. (2013) Laser Induced breakdown Spectroscopy and other analytical techniques applied on construction materials at Kom El-Dikka, Alexandria, Egypt. Mediterranean Archaeology and Archaeometry, 13, 103-119.
21. Morel, J.-C., A. Pkla, and P. Walker, Compressive strength testing of compressed earth blocks. Construction and Building Materials, 2007. 21(2): p. 303-309.
22. Othman, R., et al., Relation between Density and Compressive Strength of Foamed Concrete. Materials, 2021. 14(11).
23. Hemeda, S., Pitilakis, K. (2010). Serapeum temple and the ancient annex daughter library in Alexandria, Egypt: Geotechnical–geophysical

investigations and stability analysis under static and seismic conditions. Engineering Geology. Volume 113, Issues 1–4, Pages 33-43.
24. Atlas, R., Handbook of microbiological media, fourth edition. 2010: CRC Press.
25. Bergey's manual® of systematic bacteriology. 2005, Boston, MA: Springer US.
26. Duncan, D.B., Multiple range and multiple F tests. Biometrics, 1955. 11(1): p. 1.
27. Statistical Procedures for Agricultural Research, 2nd Edition | Wiley.
28. Costat version 6, by CoHort Software - Product details - Pubcompare.
29. Björdal, C.G. and P.K. Dayton, First evidence of microbial wood degradation in the coastal waters of the Antarctic. Scientific Reports, 2020. 10(1): p. 12774.
30. Powell, K.L., et al., Ultrastructural observations of microbial succession and decay of wood buried at a Bronze Age archaeological site. International biodeterioration & biodegradation, 2001. 47(3): p. 165-173.
31. Yue, J., et al., Study on deterioration law and mechanism of gray brick due to salt crystallization. Materials, 2022. 15(8).
32. Balksten, K. and P. Strandberg-de Bruijn, Understanding deterioration due to salt and ice crystallization in scandinavian massive brick masonry. Heritage, 2021. 4(1): p. 349-370.
33. De Weerdt, K., et al., Effect of carbonation on the pore solution of mortar. Cement and Concrete Research, 2019. 118: p. 38-56.
34. Romero-Hermida, M.I., et al., Characterization and Analysis of the Carbonation Process of a Lime Mortar Obtained from Phosphogypsum Waste. International Journal of Environmental Research and Public Health, 2021. 18(12).
35. Lamp, J.L., et al., Thermal stress weathering and the spalling of Antarctic rocks. Journal of Geophysical Research: Earth Surface, 2017. 122(1): p. 3-24.
36. Hemeda, S. (2009). Geotechnical Investigation and Seisnic Analysis of underground monuments in Alexandria, Egypt" ISO press eBooks.
37. Gao, Y., et al., Recognition of rock materials after high-temperature deterioration based on SEM Figure s via deep learning. Journal of Materials Research and Technology, 2023. 25: p. 273-284.
38. Studies on chemical elements analysis of wood using sem-edax. 2016.

39. Setyawan, E., et al. A preliminary study of scanning electron microscopy (SEM) for characterization of the wood pellet process of sengon wood (albizia chinensis). in Proceedings of the 2nd Universitas Kuningan International Conference on System, Engineering, and Technology, UNISET 2021, 2 December 2021, Kuningan, West Java, Indonesia. 2022. EAI.
40. Benavente, D., M.A. García del Cura, and S. Ordóñez, Salt influence on evaporation from porous building rocks. Construction and Building Materials, 2003. 17(2): p. 113-122.
41. Doğruyol, M., Characterization of historic mortars and the effect of rice husk ash (RHA) on quicklime. Case Studies in Construction Materials, 2024. 21: p. e03542.
42. Omar, S. and A. Kamel, Archaeometric Study of Masonry Red Bricks and Pottery Water Pipes from the Tanks of A Coptic Water Wheel, Sheikh Hamad, Athribis, Sohag, Egypt. Advanced Research in Conservation Science, 2023. 4(1): p. 18-32.
43. Building Stone Decay: From Diagnosis to Conservation. Vol. 271. 2007: Geological Society of London.
44. Elert, K., et al., Lime mortars for the conservation of historic buildings. Studies in Conservation, 2002. 47(1): p. 62-75.
45. Stone in architecture: properties, durability. 2014, Berlin, Heidelberg: Springer Berlin Heidelberg.
46. Doğruyol, M., A. Gönül, and M. Başboğa, Comparative analysis of cement-based and historic gypsum-based mortars for historical Restoration: Implications on mechanical and thermal compatibility. Journal of Building Engineering, 2025. 109: p. 112982.
47. Essential improvements in gypsum mortar characteristics. International Journal of Ecosystem, 2021. 34(2).
48. Moropoulou, A., A. Bakolas, and S. Anagnostopoulou, Composite materials in ancient structures. Cement and Concrete Composites, 2005. 27(2): p. 295-300.
49. Gaylarde, C., M. Ribas Silva, and T. Warscheid, Microbial impact on building materials: an overview. Materials and Structures, 2003. 36(5): p. 342-352.
50. Lax, S., et al., Microbial and metabolic succession on common building materials under high humidity conditions. Nature Communications, 2019. 10(1): p. 1767.

51. Jiang, L., et al., A critical review of the physiological, ecological, physical and chemical factors influencing the microbial degradation of concrete by fungi. Building and Environment, 2022. 214: p. 108925.
52. Negi, A. and I.P. Sarethy, Microbial biodeterioration of cultural heritage: events, colonization, and analyses. Microbial Ecology, 2019. 78(4): p. 1014-1029.
53. Crispim, C.A. and C.C. Gaylarde, Cyanobacteria and biodeterioration of cultural heritage: a review. Microbial Ecology, 2005. 49(1): p. 1-9.
54. Dakal, T.C. and S.S. Cameotra, Microbially induced deterioration of architectural heritages: routes and mechanisms involved. Environmental Sciences Europe, 2012. 24(1): p. 36.
55. Lippai, A., Á. Leelőssy, and D. Magyar, Indoor and outdoor air microbial contamination during different reconstruction methods of historic buildings. Pathogens (Basel, Switzerland), 2024. 13(12).
56. Scheerer, S., O. Ortega-Morales, and C. Gaylarde, Microbial deterioration of stone monuments--an updated overview. Advances in Applied Microbiology, 2009. 66: p. 97-139.
57. Ortega-Morales, B.O. and C.C. Gaylarde, Bioconservation of historic stone buildings—an updated review. Applied Sciences, 2021. 11(12): p. 5695.

Stardom University

Stardom Scientific Journal of Natural and Engineering Sciences

- Stardom Scientific Journal of Natural and Engineering Sciences -
Peer Reviewed Scientific Journal published twice
a year by Stardom University

1st issue- 4th Volume 2026

ISSN 3756-2980